HHS Public Access

Author manuscript

Ann Neurol. Author manuscript; available in PMC 2017 August 23.

Published in final edited form as:

Ann Neurol. 2015 July ; 78(1): 3–20. doi:10.1002/ana.24408.

Cerebrospinal Fluid Markers Reveal Intrathecal Inflammation in Progressive Multiple Sclerosis

Mika Komori, MD, PhD[1], **Andrew Blake, BS**[1], **Mark Greenwood, PhD**[2], **Yen Chih Lin, PhD**[1], **Peter Kosa, PhD**[1], **Danish Ghazali, BS**[1], **Paige Winokur, BS**[1], **Muktha Natrajan, MS**[1], **Simone C. Wuest, PhD**[1], **Elena Romm, MS**[1], **Anil A. Panackal, MD**[3], **Peter R. Williamson, MD, PhD**[3], **Tianxia Wu, PhD**[4], and **Bibiana Bielekova, MD**[1]

[1]Neuroimmunological Diseases Unit, National Institute of Neurological Disorders and Stroke, National Institutes of Health, Bethesda, MD

[2]Department of Mathematical Sciences, Montana State University, Bozeman, MT

[3]Translational Mycology Section, Laboratory of Clinical Infectious Diseases, National Institute of Allergy and Infectious Diseases, National Institutes of Health, Bethesda, MD

[4]Clinical Neuroscience Program, National Institute of Neurological Diseases and Stroke, National Institutes of Health, Bethesda, MD

Abstract

Objective—The management of complex patients with neuroimmunological diseases is hindered by an inability to reliably measure intrathecal inflammation. Currently implemented laboratory tests developed >40 years ago either are not dynamic or fail to capture low levels of central nervous system (CNS) inflammation. Therefore, we aimed to identify and validate biomarkers of CNS inflammation in 2 blinded, prospectively acquired cohorts of untreated patients with neuroimmunological diseases and embedded controls, with the ultimate goal of developing clinically useful tools.

Methods—Because biomarkers with maximum utility reflect immune phenotypes, we included an assessment of cell specificity in purified primary immune cells. Biomarkers were quantified by optimized electrochemiluminescent immunoassays.

Results—Among markers with cell-specific secretion, soluble CD27 is a validated biomarker of intrathecal T-cell activation, with an area under the receiver operating characteristic curve of 0.97. Comparing the quantities of cerebrospinal fluid (CSF) immune cells and their respective cell-specific soluble biomarkers (released by CSF cells as well as their counterparts in CNS tissue) provided invaluable information about stationary CNS immune responses, previously attainable via brain biopsy only. Unexpectedly, progressive and relapsing–remitting multiple sclerosis (MS)

Address correspondence to Dr Bielekova, Neuroimmunological Diseases Unit, National Institute of Neurological Disorders and Stroke, National Institutes of Health, Building 10, Room 5C103, Bethesda, MD 20892. Bibi.Bielekova@nih.gov.

Additional supporting information can be found in the online version of this article.

Potential Conflicts of Interest

Nothing to report.

patients have comparable numbers of activated intrathecal T and B cells, which are preferentially embedded in CNS tissue in the former group.

Interpretation—The cell-specific biomarkers of intrathecal inflammation may improve diagnosis and management of neuroimmunological diseases and provide pharmacodynamic markers for future therapeutic developments in patients with intrathecal inflammation that is not captured by imaging, such as in progressive MS.

The absence of reliable dynamic biomarkers of intrathecal inflammation impedes the development of specific pathobiology-based therapeutics in neuroimmunological disorders. This notion is exemplified by accelerated therapeutic developments in relapsing–remitting multiple sclerosis (RRMS) spurred by the recognition that contrast-enhancing lesions (CELs) on brain magnetic resonance imaging (MRI) reflect perivascular inflammation and therefore can serve as a sensitive, economical outcome in phase II trials of immunomodulatory treatments.[1,2] Unfortunately, CELs are rarer in progressive multiple sclerosis (MS) along with other inflammatory neurological diseases (OIND), making this biomarker less sensitive for therapeutic developments in these alternative neuroimmunological conditions. Furthermore, the past clinical success of CELs led to the false generalization that CELs are always associated with inflammation or represent all inflammatory activity. Such assumptions may lead to the administration of immunomodulatory agents to patients whose primary pathology is hypoxia or malignancy, or to the simplified (and possibly incorrect) conclusion that the immune system no longer plays a role in progressive MS. Widespread acceptance of noninvasive MRI examination as the standard diagnostic tool for MS and the limited clinical value of available cerebrospinal fluid (CSF) biomarkers[3] has fostered the tendency to perform lumbar punctures less frequently in clinical practice. An elevated immunoglobulin G (IgG) index and the presence of oligoclonal bands (OCBs), although highly prevalent in MS, are not seen in all neuroinflammatory conditions.[4] Furthermore, the longevity of plasma cells and their resistance to therapeutic interventions underlie the static nature of these traditional CSF biomarkers.[4–7] Conversely, CSF pleocytosis, although a dynamic biomarker responsive to therapeutic interventions,[8] provides unsatisfactory sensitivity and specificity ratios (Fig 1).[6] As a consequence, most difficult-to-diagnose patients end up with a brain biopsy or blind trial of immunomodulatory agents. Both methods expose patients to risks and may still lead to unsatisfactory outcomes.[9] Additionally, these approaches cannot be utilized to monitor the efficacy of applied therapies.

Hence, there remains a need for direct, dynamic biomarkers of intrathecal inflammation, ideally those that provide information about the phenotype of the inflammatory process and therefore have potential to serve as pharmacodynamic markers in drug development and bedside monitoring of therapeutic efficacy.[10] Accordingly, the purpose of this study was to develop biomarkers of intrathecal inflammation for their implementation in clinical practice and to facilitate future therapeutic developmental programs in neuroimmunological diseases characterized by a scarcity of CELs. Our aims were as follows: (1) identify candidate CSF biomarkers of intrathecal inflammation with a special emphasis on cell-specific markers (summarized in Supplementary Table); (2) optimize protocols for their quantification in CSF; (3) evaluate the cellular source(s) of these biomarkers in primary immune cells; (4)

validate the utility of consistently measurable biomarkers in CSF through blinded assessment in 2 prospectively acquired cohorts of untreated patients with neuroimmunological disorders and embedded controls; and finally, (5) explore additional insights that can be gained from the integration of biologically related biomarkers and their combinations using machine learning approaches.

Subjects and Methods

Subjects

The study was approved by the institutional review boards and all patients (or their legal guardians) signed informed consent. Subjects (Table 1) were prospectively recruited; Cohort A (n = 193) between January 2008 and 2011 and Cohort B (n = 193) after implementation of the CSF immunophenotyping protocol[11] (February 2011 to January 2014). Previously reported CSF immunophenotyping results on 153 of 193 Cohort B subjects[11] were solely used to compute combinatorial biomarkers. Eight healthy donors (HDs) were recruited through a Web portal for research study volunteers.

All subjects (including HDs) underwent a thorough diagnostic workup evaluating infectious and autoimmune causes, MRI, and CSF studies either at the National Institutes of Health (NIH; vast majority of cases) or at the referring institution. When patients were too sick to travel, CSF was couriered to the NIH from local hospitals and processed within 1 hour of ex vivo collection. For these subjects (mostly in the OIND diagnostic category), there may be missing data for IgG index and OCBs, as these tests are rarely ordered when the diagnosis of MS is not entertained. Patients did not receive central nervous system (CNS)-targeting immunomodulatory treatments for a minimum of 3 months prior to CSF collection, with the exception of a few OIND patients whose rapidly progressive clinical course was unresponsive to previously administered treatments at the outside institutions. These subjects were studied just before the next dose of their monthly immunosuppressive regimen (usually cyclophosphamide or steroids), and are over-represented in the brain biopsy cohort. Diagnoses of RRMS, secondary progressive MS (SPMS), and primary progressive MS (PPMS) were based on the 2010 McDonald criteria.[12] We classified non-MS subjects into inflammatory (OIND) and noninflammatory neurological diseases (NIND) based on the results of accepted diagnostic tests and longitudinal follow-up,[11] with one modification that the level of diagnostic certainty (ie, “definite,” “likely,” or “undiagnosed”) was recorded in the research database and updated during longitudinal follow-up. Patients with persistently low diagnostic certainty (ie, retaining “undiagnosed” classification) were excluded from the current study, which explains the higher sensitivity and specificity values for traditional diagnostic tests such as IgG index and OCBs in our cohorts. Because the NIH is a national referral center, the study is enriched in the neuroimmunological cases that are most difficult to diagnose and/or treat.

The OIND category includes patients with cryptococcal meningoencephalitis (n = 12), CNS paraneoplastic syndrome (n = 6), cyclic meningitis (n = 6), Aicardi–Goutières syndrome (AGS) with CNS involvement (n = 4), Susac syndrome (n = 3), neonatal onset multisystem inflammatory disease (NOMID) with CNS involvement (n = 2), Lyme disease with CNS involvement (n = 2), human T-cell lymphotropic virus type 1–associated myelopathy (n = 1),

sarcoidosis with CNS involvement (n = 1), CNS lupus erythematosus (n = 1), CNS vasculitis (n = 1), autoimmune lymphoproliferative syndrome with CNS involvement (n = 1), and encephalitis/ventriculitis of unknown origin (n = 5). Patients with genetic autoinflammatory diseases AGS and NOMID were included in the OIND category based on CSF pleocytosis and previously established activation of innate immunity in the CNS,[11,13,14] supported by current CSF biomarker results. The NIND group includes patients with systemic Lyme disease without CNS involvement (n = 11), systemic cryptococcosis without CNS involvement (n = 5), epilepsy (n = 5), amyotrophic lateral sclerosis (n = 3), compressive myelopathy (n = 2), leukodystrophy (n = 2), mitochondrial disease (n = 1), hydromyelia (n = 1), headache/dizziness without any CNS abnormality (n = 6), and ischemic/gliotic white matter lesions (n = 21).

CSF Collection, Processing, and Immunophenotyping

CSF was collected on ice between 9 and 11 AM and processed according to written standard operating procedures. A portion of collected CSF was sent for diagnostic workup to the NIH Clinical Center laboratory, including cell count, electrophoresis, calculations of IgG index based on comparisons of serum/CSF albumin and IgG concentrations, and presence of OCBs by isoelectric focusing (reported as nonordered patterns 1–4[15]), rapid plasma reagin, Lyme antibody, and IgG/polymerase chain reaction for selected pathogens if indicated. For the age-adjusted albumin quotient (AlbQ), age-normalized AlbQ was calculated with the following formula: measured AlbQ/(4 + age/15).[16] Research CSF aliquots were transferred to the Neuroimmunological Diseases Unit (NDU) laboratory, assigned prospective alphanumeric codes, and centrifuged at 335 × *g* for 10 minutes at 4°C within 15 minutes of collection (except when CSF was couriered to the NIH from local hospitals, in which case processing was delayed up to 1 hour postcollection). Cell pellets were 50-fold concentrated in X-VIVO 15 (Lonza, Basel, Switzerland) cultured medium and counted by hemocytometer; the number of white blood cells (WBCs) per milliliter of CSF was calculated (this enhanced CSF cell count is identified as “NDU laboratory” CSF WBC count in the results and figures). A minimum of 1×10^4 viable CSF cells were analyzed immediately by 12-color flow cytometry to enumerate absolute numbers of 14 subsets of CSF immune cells as described.[11] The CSF supernatant was aliquoted and stored in polypropylene tubes at −80°C until use.

Electrochemiluminescent Assay

Electrochemiluminescent assays were developed and optimized to quantify the concentrations of selected biomarkers in the CSF and cell culture supernatants using the Meso Scale Discovery® (MSD; Meso Scale Diagnostics, Rockville, MD) detection system. The MSD detection system provides a combination of high sensitivity with low background and a 5 log order of magnitude dynamic range.[17,18] The concentrations of interleukin (IL)-6, IL-8, and IL-12p40 were measured by MSD V-plex using the manufacturer’s protocol. The assays for IL-6R, soluble CD14 (sCD14), sCD21, sCD23, sCD27, sCD163, and C-X-C motif chemokine 13 (CXCL13) were developed in the NDU laboratory. All samples excluding IL-6, IL-8, and IL-12p40 were run in duplicate. Each assay contained a minimum of 2 additional reference samples per plate to evaluate intra- and interassay reliability.

The standard protocol for the developed assays was as follows: binding plates (MSD, L15XA) were coated with 30μl of working solution of capture antibody and stored at 4°C overnight. The next morning the coating solution was aspirated, and the plates were blocked with 150μl of 1% bovine serum albumin (BSA) in phosphate-buffered saline (PBS) pH 7.4 for 2 hours at room temperature on a shaker at 200rpm. After washing the plates 3 times with PBS–Tween-20 (PBS-T), 25μl of sample was added to each well, and the plates were incubated for 2 hours at room temperature on a shaker at 200rpm. The plates were again washed 3 times with PBS-T. Then 25μl of working solution of detection antibody was added to each well, and the plates were incubated for 2 hours at room temperature on a shaker at 200rpm. The plates were then washed 3 times with PBS-T and incubated for 1 hour with 25μl of 0.25μg/ml Sulfo-tag–labeled streptavidin solution (MSD, R32AD). Finally, the plates were washed 3 times with PBS-T, and 150μl of 2-fold concentrated Read Buffer (MSD, R92TC) were added for the SI2400 image analyzer (MSD). The standard curve was generated from a serial dilution of standard proteins in 1% BSA in PBS. The details of the reagents, manufacturer, detection limits, and intra-assay coefficients of variance are depicted in Table 2.

Assessment of Cellular Origin of Tested Biomarkers

Granulocytes, monocytes, B cells, T-cell subsets, natural killer cells, and dendritic cells (DCs) were isolated from the blood of 3 healthy donors. Granulocytes were isolated from whole blood using Polymorphprep density gradient (Axis-Shield, Dundee, UK). Other cell types were isolated via commercially available magnetic bead separation kits (Miltenyi Biotec, Bergisch Gladbach, Germany) from Ficoll gradient-treated apheresis samples. Purified cells were cultured at a concentration of 1×10^6 cells/ml in serum-free X-VIVO 15 medium (Lonza) in the presence or absence of 10μg/ml phorbol myristate acetate and 1μM Ionomycin. Supernatants were collected after 48 hours and frozen until biomarker measurements were taken. The concentration of biomarker per specific immune cell type was calculated using flow cytometry–derived purity data obtained before each cell culture.

Immunohistochemistry

CNS autopsy or biopsy tissue sections from nonimmunocompromised cryptococcal meningoencephalitis patients (different from patients included in the biomarker cohort) and selected patients with undiagnosed possibly neuroimmunological CNS conditions were analyzed by immunohistochemistry. Paraffin-embedded sections were immunostained with mouse antihuman monoclonal antibodies against CD3 (clone F7.2.38; Dako, Carpinteria, CA), CD4 (1F6; Novocastra/Leica Biosystems, Buffalo Grove, IL), CD8 (C8/144B; Dako), and CD68 (clone KP1; Dako). Signals were detected by horseradish peroxidase–conjugated secondary antibody using an automated chromogenic detection system. The images were obtained by Leica AF 6000 LX and Leica Epi camera microscope with LAS AF version 4.0.0 software (Leica Microsystems) for Figure 2E and F, and Aerio ImageScope version 12.1.0.5029 (Leica Biosystems) for Figure 2G and H, without any postacquisition modification of contrast or brightness.

MRI and CEL Counting

Routine spin-echo and gradient-echo T1-weighted images were collected following intravenous administration of 0.1mmol/kg gadopentetate dimeglumine as described.[19] CELs were quantified according to the consensus of 2 neurologists with neuroimmunology subspecialty training (B.B. and M.K.) based on precontrast T1- and T2-weighted images.

Statistical Analyses

To evaluate associations between biomarkers and diagnoses, 1-way analysis of variance (ANOVA) and Fisher exact test were performed. In the ANOVA, each continuous biomarker was tested for each of the 3 data sets: Cohort A, Cohort B, and the 2 cohorts combined, and for each of the 2 diagnostic variables: the first diagnosis variable with 6 levels (RRMS, PPMS, SPMS, NIND, HD, and OIND; Figs 1–4), and the other with 2 levels (cyclic meningitis and cryptococcal meningoencephalitis; see Fig 2). Tukey's method was used for pairwise multiple comparisons. In Fisher exact test, the continuous biomarkers were dichotomized using mean + 2 standard deviation (SD) or the third quartile (Q3) + 1.5 interquartile range (IQR; for CXCL13 only) as thresholds, where mean, SD, Q3, and IQR were calculated from HD subjects' nontransformed data. For CELs, 0 was used as the threshold.

To evaluate the accuracy of the test, the area under the receiver operating characteristic (ROC) curve (AUC) was calculated using 2 dichotomized diagnosis variables: patients with (OIND + PPMS + RRMS + SPMS) versus without (HD + NIND) intrathecal inflammation (see Figs 1, 3, 4) and patients with progressive MS (SPMS + PPMS) versus RRMS (see Fig 2). AUCs from binary predictors (OCB pattern 2: present or absent and OCB pattern 2 or 3: present or absent) were also estimated (table in Fig 1). Bootstrap methods were used to calculate confidence intervals (CIs) for the AUC and to compare the different ROC models (DeLong method) based on the pROC package in R.[20] The correlation between biomarker variables was evaluated by Pearson correlation coefficients (Fig 5). R 3.1.2 or SAS version 9.2 (SAS Institute, Cary, NC) was used for above analyses.

Machine learning (or artificial intelligence) tools are used to identify patterns among multiple biomarkers and variables useful for predicting inflammation that may not be readily visible using traditional statistical analyses. By combining complex information from multiple biomarkers measured in each individual, it should be possible to build a better class predictor than can be achieved using a single biomarker. Gradient boosting machines (GBM)[21] are the machine learning techniques employed because of their known excellent predictive ability, because they allow for both additive and interactions effects for predictors, and because of the way they handle missing predictor variables, which were encountered for some of the IgG index data in the OIND cohort and occasionally for other predictors. GBM involves a weighted combination of a large set of small (4 nodes here) sequential classification trees,[22] improving on a single tree with additional trees fit to the sequential residuals. The classifiers were trained on a subset of the observations using the "gbm" R package,[23] selecting the optimal number of trees using cross-validation with a conservative learning rate of 0.001. The predictive ability of the trained classifiers was assessed on the withheld (validation) data set.[24] Other related statistical methods such as logistic regression,

multinomial logistic regression, and random forests could also have been used, but their missing data handling requires either imputation of missing predictors or deletion of any responses containing a missing predictor variable response. Because there is not a single tree output, GBM results are more complicated to explore. Three aspects of GBM are informative: the first is variable importance, a general measure of the relative utility of each variable to explain variation in the responses; the second is the estimated marginal effects of each predictor to understand the role of important predictors on the predicted responses; the third is the predictive performance of the model on withheld observations—the real test of any classifier. To support the benefits of using GBM, the classification performance on withheld observations is compared to the results for a single classification tree that was pruned using cross-validation.

Results

To compare new biomarkers with those currently available in clinical practice, we provide results in Figure 1 for IgG indices, CSF WBC counts, AlbQs, and CELs with their respective ROC curves. AUCs were generated for all ROCs as well as for 2 binary versions of OCB patterns based on the estimated sensitivity and specificity results (for pattern 2 OCB: present or absent and patterns 2 or 3 OCB: present or absent). Please note that because these traditional diagnostic tests played a role in diagnostic classification and categorization of the level of certainty for diagnostic conclusions (see Subjects and Methods), our sensitivity and specificity values outperform previously reported studies,[4] as we specifically excluded subjects with discordant diagnostic conclusions and traditional laboratory biomarkers (such as HDs with positive OCBs).

After unblinding, the corresponding diagnostic categories in the 2 separate cohorts yielded consistent results for all reproducibly measured novel biomarkers. Therefore, we provide data in Figures 1, 3, and 4 for the combined (n = 386) data set and describe in the text and figure legends the important differences observed between Cohorts A and B.

Among Cytokines and Chemokines, IL-12p40 and IL-8 Consistently Differentiate Inflammatory from Noninflammatory Subgroups

The chemokine IL-8, mainly produced by activated cells of the innate immune system (see Fig 3A), consistently differentiated OIND from all other diagnoses (see Fig 3B). The chemokine CXCL13, secreted by activated T cells and DCs, was also dependably elevated in OIND patients, whereas its increased levels in RRMS and SPMS did not reach significance in the validation cohort. Of the cytokines tested, IL-6 and its soluble receptor (IL-6Ra) were ubiquitously produced by different immune cells. These related markers were elevated only in the confirmatory cohort of OIND patients. Conversely, IL-12p40, released by activated DCs and to a lesser degree by activated $CD8^+$ T cells and B cells, was consistently elevated in the OIND, RRMS, and SPMS cohorts. IL-12p40 differentiated PPMS from RRMS in both cohorts, but from SPMS only in 1 cohort.

Soluble Surface Markers Have Restricted Cellular Origins and Provide Added Clinical Value

Whereas sCD14 is a specific monocyte marker, sCD163 is released by both monocytes and DCs in resting and activated states (see Fig 4A). Consequently, sCD14 and sCD163 were highly correlated ($r_{Pearson} = 0.795$, $p < 0.0001$; see Fig 5) and reproducibly differentiated OIND from other diagnoses (see Fig 4B). Although sCD14 was also elevated in progressive MS in comparison to NIND and RRMS patients in both cohorts, the difference in the confirmatory cohort did not reach statistical significance.

Soluble CD21 is a selective biomarker of B cells released in resting and activated states (see Fig 4A). Although its levels were elevated in the OIND and all MS groups in comparison to the NIND group, the only statistically significant difference in the confirmatory cohort occurred between OIND and NIND patients (see Fig 4B). Given our verification that CD21 expression by B cells decreases during differentiation (data not shown), we sought to develop more reliable memory B-cell–specific biomarkers by measuring sCD19, sCD20, and sCD23. Whereas CSF levels of sCD19 and sCD20 were below the detection limit of our assays (see Table 2), sCD23 was released by many cell types, and thereby lacked discriminatory power (see Fig 4).

Although expressed by several cell types (especially T and B cells), sCD27 was secreted in large quantities only by activated T cells, CD8>CD4. sCD27 reproducibly differentiated all neuroimmunological diseases from NIND patients and HDs with an exceptional AUC (0.97, 95% CI = 0.96–0.99; see Fig 4).

Combined Biologically Related Biomarkers Yield Insight into Immune Responses in CNS Tissue

CSF inflammatory biomarkers are released from all intrathecal immune cells including those in the CSF and CNS tissue. Because HDs lack pathological immune infiltration of the CNS, the ratio of cell-specific biomarkers to CSF-resident cells in HDs indicates the limits of physiological secretion by mobile, CSF immune cells. Ratios higher than the HD range imply that CSF cells cannot fully account for the biomarker measured. The excess soluble biomarkers suggest a pool of intrathecal immune cells embedded in the CNS tissue and therefore unaccounted for by CSF immunophenotyping.

To test this hypothesis, we calculated 3 combinatorial biomarkers in Cohort B: ratios of sCD14/monocyte, sCD21/B cell, and sCD27/T cell, each measured per milliliter of CSF (see Fig 2A). We observed that the sCD14/monocyte ratio did not differ among diagnostic groups, whereas the sCD21/B-cell and especially sCD27/T-cell ratios did. Surprisingly, the sCD27/T-cell ratio was significantly higher in progressive MS patients compared to all other diagnostic groups. sCD21/B-cell and sCD27/T-cell ratios differentiated progressive MS from RRMS patients based on an AUC that is comparable to current clinically utilized tests (AUC = 0.76–0.77; see Fig 2B).

Because OIND is a heterogeneous category, we extracted 2 diagnostically homogeneous groups to test our inference that the ratio of soluble biomarker per cell of origin can identify patients with immune cell infiltration in CNS tissue. Patients with cyclic meningitis suffer

from years of cyclic headaches and meningeal signs, but do not accumulate neurological disability. Immunocompetent patients with cryptococcal meningoencephalitis have prominent CSF pleocytosis, and some also have CNS infiltration by immune cells as evidenced by brain MRI abnormalities and neurological dysfunction. Both meningitis cohorts had elevated sCD14, sCD21, and sCD27 CSF levels (see Fig 2C). However, the first group exhibited normal combinatorial ratios, demonstrating that their CSF cells fully accounted for the production of soluble biomarkers. In contrast, the sCD14/monocyte ratio was elevated in the majority of cryptococcal meningoencephalitis patients, indicating that the excess CSF sCD14 likely originated from monocytes or microglia in the CNS. sCD27/T-cell ratios were also elevated in some of these patients, suggesting the accumulation of T cells in the CNS (see Fig 2D). Dominant monocyte or microglial activation and variable T-cell infiltration are characteristics of brain autopsy specimens from immunocompetent patients with cryptococcal meningoencephalitis (see Fig 2E, F).

We further tested the performance of new biomarkers in the subcohort of difficult-to-diagnose patients whose diagnostic workup included brain biopsies or who had postmortem examinations of CNS tissue. Upon query of our research database, we identified 14 subjects with CNS pathology results: 1 with NIND (presumably mitochondrial encephalopathy with lack of inflammatory cells on brain biopsy other than activated microglia), 1 with PPMS (died of stroke but pathology was consistent with longstanding MS, including perivascular and tissue lymphocytic infiltrates), and 12 with OIND. sCD27 correctly identified the presence or absence of CNS inflammation in 100% (14 of 14) of cases, in contrast to CSF WBC count (correct in 6 of 14 cases, 42.9%), CELs (correct in 8 of 13 cases, 61.5%, if we included meningeal inflammation under the CELs category), IgG index (correct in 1 of 9 cases, 11.1%; only the PPMS case had a positive IgG index and the remaining 8 OIND patients in whom the test was ordered had normal IgG indices), and OCB (correct in 3 of 9 cases, 33.3%; the PPMS case and 2 OIND cases). We include pathology from the most illustrative patient (see Fig 2G, H), who had no CELs, a normal IgG index (0.58), pattern 1 OCBs (ie, no OCBs in the blood or CSF), and a normal CSF WBC count (1 cell per μl). However, he had elevated CSF sCD27 (19.4U/ml), sCD14 (157.5ng/ml), sCD163 (58.8ng/ml), and IL-12p40 (13.6pg/ml). The autopsy demonstrated rich lymphohistiocytic infiltrate, consisting mostly of $CD3^+/CD8^+$ T cells and KP1-positive histiocytes or microglial cells present in leptomeninges and perivascular and intraparenchymal areas involving multiple (but not all) sampled areas of frontal and parietal lobes, cerebellum, and spinal cord. Myelin pallor, without definite demyelination, axonal injury, and reactive gliosis were also present. The final diagnosis was delayed graft versus host disease with inflammatory encephalopathy, and the cause of death was hypercarbic respiratory failure.

Novel Inflammatory Biomarkers Differentiate Patients with Diverse Phenotypes of Intrathecal Inflammation

Classification trees and GBM (see Subjects and Methods) were considered for 2 modeling problems: predicting the presence or absence of intrathecal inflammation (which can be directly compared to the performance of sCD27), and the development of a 5-class diagnostic predictor (ie, HD+NIND [which were merged into a single category because of a small number of HDs], RRMS, PPMS, SPMS, and OIND). In predicting intrathecal

inflammation, sCD27 clearly dominated the classifier with a relative importance >20-fold higher than any remaining variable (Fig 6A). In the training data set, the GBM model had an AUC of nearly 1 (0.9987), showing nearly perfect classification. In the validation data set, the AUC was 0.97. The model never predicts inflammation for a subject without inflammation, but fails to predict inflammation in 17 of 162 subjects (10%) clinically classified into the OIND or MS categories (data not shown). The GBM model performed slightly better than a single pruned classification tree (validation data set AUC = 0.95), which split the responses based on sCD27 values of 11.1 (results not shown).

In the 5-category GBM classifier, sCD27 was still the most important variable; however, many additional variables, including age-normalized AlbQ, 2 related biomarkers of myeloid lineage (sCD163 and sCD14), IgG index, IL-6, NDU laboratory optimized CSF WBC count (see Subjects and Methods), and IL-12p40, had considerable importance in distinguishing different diagnostic categories within patients showing intrathecal inflammation (see Fig 6B). In contrast, the most promoted biomarkers in RRMS research, CELs and CXCL13, ranked as the least important discriminatory variables. The accuracy of the 5-class GBM discriminator in the training cohort was 0.95 (95% CI = 0.91–0.98; McNemar test $p < 0.0001$), whereas the model's accuracy in the validation data set dropped to 0.55 (95% CI = 0.48–0.63; McNemar test $p < 0.0001$). The similar pruned classification tree had an accuracy of 43% for the validation data. The confusion matrix (table of predicted and true values) for the GBM for the validation cohort (see Fig 6C) demonstrated perfect prediction for the NIND+HD category, but incorrectly classified at least a few subjects from all remaining diagnostic groups. As expected, the classifier had difficulties distinguishing between MS subtypes and quite expectedly classified as HD+NIND approximately 10% of subjects who lacked elevated inflammatory biomarkers despite belonging to the MS or OIND categories based on clinical evaluation. The estimated marginal effects of important predictors (results not shown) show that sCD27 focuses on discriminating HD+NIND versus other categories. Age-normalized AlbQ shows a small decrease in the predicted probability of PPMS for values > 1.25 and a slight increase in the predicted probability of OIND with increasing values of the predictor. Similarly, sCD163 shows an estimated effect that includes an increased probability of OIND for values > 30. In addition, sCD14 shows an increased probability of SPMS for values 50. The latter effects are related to variables of lesser importance, and are subtle as well as challenging to assess in the context of simultaneous predicted probabilities for the 5 categories. Please note that we could not test the performance of ratios of cell-specific soluble biomarkers divided by cells of origin in machine learning discriminators, as these combinatorial biomarkers were only available for the validation cohort.

Discussion

Although IgG index and OCBs have been invaluable markers of intrathecal activation of humoral immunity in MS, they are absent in many OIND conditions. Due to the longevity of plasma cells, these biomarkers can persist years after the inflammatory insult has subsided. Conversely, cell counts from unspun CSF are insensitive to mild to moderate levels of inflammation.[11] Although novel biomarkers of active intrathecal inflammation have been proposed,[25–30] none of them has been implemented in clinical practice.[31] Several plausible

reasons include a perceived or actual lack of experimental rigor; the absence of validation in blinded, prospectively acquired cohort(s); and sparse evidence that new biomarkers offer additional clinical value. Our goal in the current study was to address all of these issues.

Ten of 19 candidate biomarkers (see Table 2) were detectable in CSF. Consistent with our hypothesis, shed surface markers were associated with a restricted cellular origin in comparison to cytokines/chemokines. Although CXCL13 has been considered the most useful novel biomarker in MS thus far,[25,31–33] IL-12p40 was found in the present study to have a partially overlapping cellular origin, was detectable in all CSF samples, and differentiated the MS subtypes. Thus, the present data suggest that IL-12p40 is the most valuable biomarker among the cytokines/chemokines tested. In addition to IL-12p40, IL-8 was found to be useful in distinguishing MS from OIND patients.

Soluble CD27 was found to be the best single biomarker of active intrathecal inflammation. This conclusion was supported by machine learning algorithms that consistently ranked sCD27 as the most important discriminatory biomarker for all classifiers. Formal statistical analysis demonstrated the superiority of sCD27 (AUC = 0.97) in comparison to the IgG index (AUC = 0.92) with bootstrap $p = 0.0012$, and to OCB pattern 2 (AUC = 0.83) with $p < 0.0001$, but provided no evidence of a difference when compared to combined OCB patterns 2 or 3 (AUC = 0.96) with $p = 0.136$. Considering that we excluded individuals with low levels of diagnostic certainty (most often based on discrepancies between clinical diagnoses and traditional laboratory tests) and therefore sensitivity and specificity data for traditional CSF biomarkers in our cohorts were generally higher than previously reported,[4,6] the reliability of sCD27 was outstanding. This conclusion is supported by a 100% concordance with the pathological diagnosis in 14 cases with available CNS biopsy or autopsy, whereas the combination of all existing biomarkers could correctly identify only 61.5% of cases.

Although expressed on multiple immune cells, sCD27 is shed in highest concentrations by activated T cells. In light of the numerical predominance of T cells in the CSF, we considered contributions from alternative sources to be negligible. Thus, the correlation between sCD27 levels and absolute numbers of CSF T cells ($r_{\text{Pearson}} = 0.523$, $p < 0.0001$; see Fig 5) supports our conclusion that sCD27 is an excellent biomarker of T-cell–mediated inflammation.

Although the other inflammatory biomarkers tested were not useful diagnostic predictors on their own, sCD21 and sCD14/sCD163 provided valuable information about immune phenotype, which proved to be useful in the more complicated GBM classifiers. Despite the selective release of sCD21 by B cells, its expression decreased during the maturation process. Consequently, high sCD21 levels indicate intrathecal expansion of B cells, yet normal sCD21 values do not exclude it. Hence, although not an ideal diagnostic biomarker, its specificity for B cells makes sCD21 a useful pharmacodynamic marker for B-cell–depleting therapies in personalized medicine paradigms.

Soluble CD14 is selectively released by monocytes, presumably during the differentiation process. Because activated microglia also express CD14,[34] it may be the main producer of CSF sCD14. The weak correlation between sCD14 levels and CSF monocyte counts (r_{Pearson}

= 0.272, $p = 0.0002$, see Fig 5) supports this interpretation. Accordingly, elevated sCD14 levels and especially sCD14/monocyte ratios may represent novel markers of microglial activation. As microglial activation has been reported in many conditions (both inflammatory and noninflammatory) and aging,[35,36] it is noteworthy that ~30% of patients with all diagnoses were associated with elevated sCD14/monocyte ratios, and that age explained some of this biomarker's variance ($r_{Pearson} = 0.333$, $p < 0.0001$; see Fig 5).

Whereas current clinical practice entails evaluating each laboratory test in isolation, we have argued[37] that a thoughtful combination of biologically related measurements can lead to new insights. Investigating the cellular origin of biomarkers is the simplest application of this systems biology principle. Thus, comparing the numbers of CSF cells with the marker(s) they secrete reveals information about immune cells embedded in CNS tissue. Excellent concordance between combinatorial cell-specific biomarkers and pathological observations in the current study suggests that the described methodology has the potential to replace brain biopsies. At the minimum, it represents a practical tool for longitudinal assessment of CNS inflammation in the therapeutic management of patients with neuroimmunological diseases that are not associated with CELs. Although this cross-sectional study does not provide evidence for the dynamic nature of the biomarkers studied, published longitudinal studies, either in the CSF or blood (in systemic inflammatory conditions) document their correlation with the severity of inflammatory processes and their responses to immunomodulatory treatments.[30,38] We confirmed the dynamic nature of these biomarkers in anecdotal observations during therapeutic management of some of the most difficult-to-treat OIND patients (data not shown), and plan to formally validate these biomarkers as pharmacodynamic markers in ongoing clinical trials (NCT01212094 and NCT01143441).

Validation of the 5-group GBM classifier demonstrated that it is not possible to distinguish the selected diagnostic categories with an overall accuracy >60% based on the studied inflammatory biomarkers. Because immune biomarkers are well defined in their measuring capabilities (eg, sCD27 being specific for activated T cells, sCD21 for B cells, sCD14 for monocytes or microglia, and none secreted by nonimmune CNS cells), this biomarker classifier is by definition more precise in measuring intrathecal inflammation than any clinical classifier. Our data show that although the overall "bulk" of intrathecal inflammation is comparable between the 3 MS subgroups, approximately 10% of patients in each MS diagnostic category lack intrathecal inflammation. These data are highly reminiscent of pathology studies that identified a small subgroup of MS subjects who develop acute demyelinating lesions by mechanisms other than T-cell or B-cell/antibody-mediated inflammation (ie, type 3 and type 4 in Lucchinetti's classification).[39] We propose that these rare MS patients can now be identified without brain biopsy based on CSF biomarker panels.

The surprising observation that patients with both progressive MS subgroups have comparable levels of many inflammatory biomarkers to RRMS patients but that sCD27/T-cell ratios were elevated selectively in progressive MS groups indicates that T-cell infiltration of the CNS is a hallmark of progressive MS, without clear distinction between PPMS and SPMS subtypes. This finding contradicts the prevailing notion that inflammation no longer plays a pathogenic role in progressive MS as deduced from the lack of CELs and failure of current immunomodulatory treatments to inhibit disease progression. Weak

correlations ($r < 0.27$; see Fig 5) observed between CELs and soluble cell surface markers in this study confirm that CELs only reflect inflammation that disrupts the blood–brain barrier. Whereas such perivascular inflammation is infrequent, T-cell infiltration of brain tissue is consistently present in progressive MS.[40,41] Why then do immunomodulatory treatments fail?[42] Although a possible explanation is that intrathecal inflammation, although present, no longer drives progression of disability, there is actually no pharmacodynamic proof that any of the tested therapies ablated compartmentalized CNS inflammation in progressive MS. Available pathological evidence[30,43,44] demonstrates that even strong immunosuppression followed by autologous bone marrow transplant failed to do so. This counterintuitive phenomenon emphasizes the need for verification of the therapeutic efficacy in the intrathecal compartment using pharmacodynamic markers such as those presented here. Furthermore, it underscores that we can exclude a contributory role of CNS inflammation in progressive MS only if we successfully abolish compartmentalized inflammation and observe no effect on the accumulation of disability.

Previously published functional data indicate that intrathecal T cells in progressive MS have phenotypes of terminally differentiated cells,[45] making them resistant to immunosuppressive agents that target cells in the proliferation cycle. Together with insight obtained from the current paper, we conclude that the observed lack of efficacy of current therapeutic agents in progressive MS may be due to inadequate penetrance of large molecules (such as biologicals) to CNS tissue and preferential targeting of proliferating cells by small molecules, such as classical immunosuppressive/cancer therapeutics. Our data predict that effective inhibition of intrathecal inflammation in progressive MS could require agents with excellent CNS penetrance that target immune effector functions such as cytotoxicity and cytokine secretion, rather than proliferation.

Although their usefulness must be proven in future longitudinal studies, the described combinatorial CSF biomarkers may facilitate the screening of such novel immunomodulatory therapies for progressive MS in economical phase II trials by stratifying cohorts for subjects with therapeutic targets and allowing for a baseline versus treatment study design providing evidence of efficacy on selected biomarker(s) in periods as short as 3 to 6 months. Although only subsequent phase III trials can offer proof of a drug’s efficacy on disability, combinations of biomarkers and clinical data may validate surrogacy (or predictive value) of the biomarker for clinical outcome, which would open the era of rational personalized medicine to the neuroimmunology field.

Supplementary Material

Refer to Web version on PubMed Central for supplementary material.

Acknowledgments

This work was supported by the intramural research program of the NIH National Institute of Neurological Disorders and Stroke and by the intramural research program of the NIH National Institute of Allergy and Infectious Diseases. M.K. received postdoctoral fellowship support from the Japan Society of the Promotion of Science.

We thank clinicians I. Cortese, J. Ohayon, K. Fenton, C. Toro, D. Landis, A. Vanderver, E. Wells, J. Cherup, and A. Wichman, and research nurses H. Griffith and J. Dwyer for expert patient care; A. Mayfield for patient scheduling and support; and S. Pittaluga, M. Quezado, and A. Ray-Chaudhury for helping with histopathological analysis.

References

1. Sormani MP, Bruzzi P. MRI lesions as a surrogate for relapses in multiple sclerosis: a meta-analysis of randomised trials. Lancet Neurol. 2013; 12:669–676. [PubMed: 23743084]
2. Filippi M, Rocca MA, Barkhof F, et al. Association between pathological and MRI findings in multiple sclerosis. Lancet Neurol. 2012; 11:349–360. [PubMed: 22441196]
3. Stangel M, Fredrikson S, Meinl E, et al. The utility of cerebrospinal fluid analysis in patients with multiple sclerosis. Nat Rev Neurol. 2013; 9:267–276. [PubMed: 23528543]
4. Petzold A. Intrathecal oligoclonal IgG synthesis in multiple sclerosis. J Neuroimmunol. 2013; 262:1–10. [PubMed: 23890808]
5. Axelsson M, Mattsson N, Malmestrom C, et al. The influence of disease duration, clinical course, and immunosuppressive therapy on the synthesis of intrathecal oligoclonal IgG bands in multiple sclerosis. J Neuroimmunol. 2013; 264:100–105. [PubMed: 24125567]
6. Link H, Huang YM. Oligoclonal bands in multiple sclerosis cerebrospinal fluid: an update on methodology and clinical usefulness. J Neuroimmunol. 2006; 180:17–28. [PubMed: 16945427]
7. Bonnan M. Intrathecal IgG synthesis: a resistant and valuable target for future multiple sclerosis treatments. Mult Scler Int. 2015; 2015:296184. [PubMed: 25653878]
8. Stuve O, Marra CM, Jerome KR, et al. Immune surveillance in multiple sclerosis patients treated with natalizumab. Ann Neurol. 2006; 59:743–747. [PubMed: 16634029]
9. Gelfand JM, Genrich G, Green AJ, et al. Encephalitis of unclear origin diagnosed by brain biopsy: a diagnostic challenge. JAMA Neurol. 2015; 72:66–72. [PubMed: 25365755]
10. Bielekova B, Martin R. Development of biomarkers in multiple sclerosis. Brain. 2004; 127(pt 7): 1463–1478. [PubMed: 15180926]
11. Han S, Lin YC, Wu T, et al. Comprehensive immunophenotyping of cerebrospinal fluid cells in patients with neuroimmunological diseases. J Immunol. 2014; 192:2551–2563. [PubMed: 24510966]
12. Polman CH, Reingold SC, Banwell B, et al. Diagnostic criteria for multiple sclerosis: 2010 revisions to the McDonald criteria. Ann Neurol. 2011; 69:292–302. [PubMed: 21387374]
13. Crow YJ, Rehwinkel J. Aicardi-Goutieres syndrome and related phenotypes: linking nucleic acid metabolism with autoimmunity. Hum Mol Genet. 2009; 18:R130–R136. [PubMed: 19808788]
14. Rodriguez-Smith J, Lin Y, Kim H, et al. A173: Cerebrospinal fluid cytokines correlate with innate immune cells in neonatal onset multisystem inflammatory disease (NOMID) patients in clinical remission treated with anakinra. Arthritis Rheumatol. 2014; 66(suppl 11):S226.
15. Freedman MS, Thompson EJ, Deisenhammer F, et al. Recommended standard of cerebrospinal fluid analysis in the diagnosis of multiple sclerosis: a consensus statement. Arch Neurol. 2005; 62:865–870. [PubMed: 15956157]
16. Reiber H, Padilla-Docal B, Jensenius JC, Dorta-Contreras AJ. Mannan-binding lectin in cerebrospinal fluid: a leptomeningeal protein. Fluids Barriers CNS. 2012; 9:17. [PubMed: 22889364]
17. Tighe P, Negm O, Todd I, Fairclough L. Utility, reliability and reproducibility of immunoassay multiplex kits. Methods. 2013; 61:23–29. [PubMed: 23333412]
18. Leng SX, McElhaney JE, Walston JD, et al. ELISA and multiplex technologies for cytokine measurement in inflammation and aging research. J Gerontol A Biol Sci Med Sci. 2008; 63:879–884. [PubMed: 18772478]
19. Bielekova B, Kadom N, Fisher E, et al. MRI as a marker for disease heterogeneity in multiple sclerosis. Neurology. 2005; 65:1071–1076. [PubMed: 16217061]
20. Robin X, Turck N, Hainard A, et al. pROC: an open-source package for R and S+ to analyze and compare ROC curves. BMC Bioinformatics. 2011; 12:77. [PubMed: 21414208]
21. Friedman JH. Greedy function approximation: a gradient boosting machine. Ann Stat. 2001; 29:1189–1232.

22. Breiman, L., Friedman, J., Olshen, R., Stone, C. Classification and regression trees. Belmont, CA: Wadsworth; 1984.
23. Ridgeway G. gbm: generalized boosted regression models. R package. 2.1. 2013 ed.
24. James, G., Witten, D., Hastie, T., Tibshirani, R. An introduction to statistical learning: with applications in R. New York, NY: Springer; 2013.
25. Sellebjerg F, Bornsen L, Khademi M, et al. Increased cerebrospinal fluid concentrations of the chemokine CXCL13 in active MS. Neurology. 2009; 73:2003–2010. [PubMed: 19996075]
26. Desplat-Jego S, Feuillet L, Pelletier J, et al. Quantification of immunoglobulin free light chains in cerebrospinal fluid by nephelometry. J Clin Immunol. 2005; 25:338–345. [PubMed: 16133990]
27. Comabella M, Fernandez M, Martin R, et al. Cerebrospinal fluid chitinase 3-like 1 levels are associated with conversion to multiple sclerosis. Brain. 2010; 133(pt 4):1082–1093. [PubMed: 20237129]
28. Khademi M, Dring AM, Gilthorpe JD, et al. Intense inflammation and nerve damage in early multiple sclerosis subsides at older age: a reflection by cerebrospinal fluid biomarkers. PloS One. 2013; 8:e63172. [PubMed: 23667585]
29. Duan H, Luo Y, Hao H, et al. Soluble CD146 in cerebrospinal fluid of active multiple sclerosis. Neuroscience. 2013; 235:16–26. [PubMed: 23333866]
30. Mondria T, Lamers CH, te Boekhorst PA, et al. Bone-marrow transplantation fails to halt intrathecal lymphocyte activation in multiple sclerosis. J Neurol Neurosurg Psychiatry. 2008; 79:1013–1015. [PubMed: 18223013]
31. Comabella M, Montalban X. Body fluid biomarkers in multiple sclerosis. Lancet Neurol. 2014; 13:113–126. [PubMed: 24331797]
32. Khademi M, Kockum I, Andersson ML, et al. Cerebrospinal fluid CXCL13 in multiple sclerosis: a suggestive prognostic marker for the disease course. Mult Scler. 2011; 17:335–343. [PubMed: 21135023]
33. Krumbholz M, Theil D, Cepok S, et al. Chemokines in multiple sclerosis: CXCL12 and CXCL13 up-regulation is differentially linked to CNS immune cell recruitment. Brain. 2006; 129(pt 1):200–211. [PubMed: 16280350]
34. Ulvestad E, Williams K, Mork S, et al. Phenotypic differences between human monocytes/macrophages and microglial cells studied in situ and in vitro. J Neuropathol Exp Neurol. 1994; 53:492–501. [PubMed: 8083690]
35. Luo XG, Ding JQ, Chen SD. Microglia in the aging brain: relevance to neurodegeneration. Mol Neurodegener. 2010; 5:12. [PubMed: 20334662]
36. Olsson B, Hertze J, Lautner R, et al. Microglial markers are elevated in the prodromal phase of Alzheimer's disease and vascular dementia. J Alzheimer Dis. 2013; 33:45–53.
37. Bielekova B, Vodovotz Y, An G, Hallenbeck J. How implementation of systems biology into clinical trials accelerates understanding of diseases. Front Neurol. 2014; 5:102. [PubMed: 25018747]
38. Huang J, Jochems C, Anderson AM, et al. Soluble CD27-pool in humans may contribute to T cell activation and tumor immunity. J Immunol. 2013; 190:6250–6258. [PubMed: 23677477]
39. Lucchinetti C, Bruck W, Parisi J, et al. Heterogeneity of multiple sclerosis lesions: implications for the pathogenesis of demyelination. Ann Neurol. 2000; 47:707–717. [PubMed: 10852536]
40. Hauser SL, Bhan AK, Gilles F, et al. Immunohistochemical analysis of the cellular infiltrate in multiple sclerosis lesions. Ann Neurol. 1986; 19:578–587. [PubMed: 3524414]
41. Booss J, Esiri MM, Tourtellotte WW, Mason DY. Immunohistological analysis of T lymphocyte subsets in the central nervous system in chronic progressive multiple sclerosis. J Neurol Sci. 1983; 62:219–232. [PubMed: 6607973]
42. Koch MW, Cutter G, Stys PK, et al. Treatment trials in progressive MS—current challenges and future directions. Nat Rev Neurol. 2013; 9:496–503. [PubMed: 23897406]
43. Metz I, Lucchinetti CF, Openshaw H, et al. Autologous haematopoietic stem cell transplantation fails to stop demyelination and neurodegeneration in multiple sclerosis. Brain. 2007; 130(pt 5): 1254–1262. [PubMed: 17293360]

44. Lu JQ, Storek J, Metz L, et al. Continued disease activity in a patient with multiple sclerosis after allogeneic hematopoietic cell transplantation. Arch Neurol. 2009; 66:116–120. [PubMed: 19139309]

45. Wuest SC, Mexhitaj I, Chai NR, et al. A complex role of herpes viruses in the disease process of multiple sclerosis. PLoS One. 2014; 9:e105434. [PubMed: 25148387]

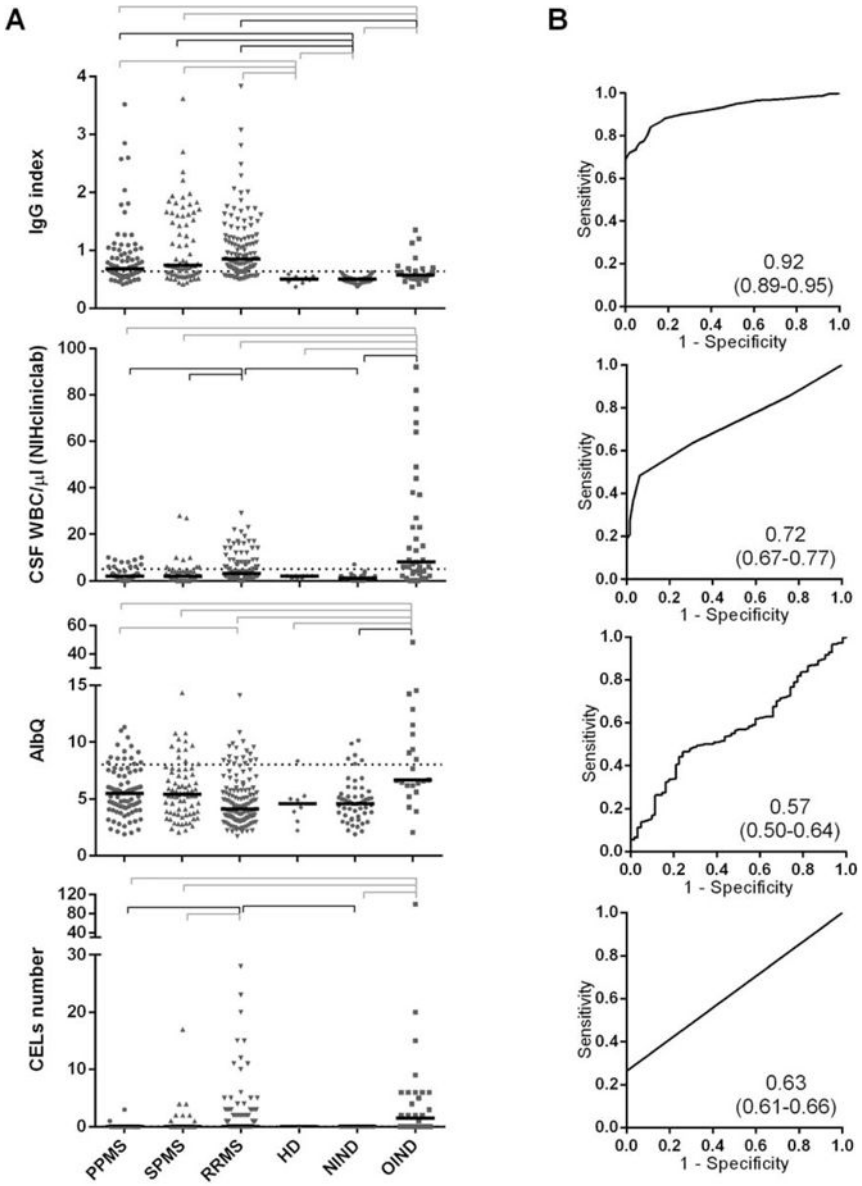

	Sensitivity (95% CI)	Specificity (95% CI)	AUC (95%CI)
OCB pattern 2	0.66 (0.60-0.72)	1 (0.93-1)	0.83 (0.80-0.86)
OCB pattern 2 or 3	0.93 (0.89-0.95)	0.98 (0.90-1)	0.95 (0.93-0.98)

FIGURE 1.

Validation of traditional biomarkers for intrathecal inflammation. (A) Traditional intrathecal inflammatory biomarkers, including immunoglobulin G (IgG) index, white blood cell (WBC) counts in unspun cerebrospinal fluid (CSF; CSF WBC/µl; NIH clinical laboratory), albumin quotient (AlbQ), number of contrast-enhancing lesions (CELs) on brain magnetic resonance imaging performed at the time of lumbar puncture, and oligoclonal bands (OCBs), were validated in coded CSF samples of combined Cohorts A and B (n = 386). Primary progressive multiple sclerosis (PPMS), secondary progressive MS (SPMS), relapsing–remitting MS (RRMS), healthy donors (HD), noninflammatory neurological

diseases (NIND), and other inflammatory neurological diseases (OIND) were compared between each diagnostic category. OCB type 2 represents OCBs in CSF but not in serum, indicative of isolated intrathecal oligoclonal IgG synthesis. OCB type 3 represents identical OCBs in the CSF and serum plus additional, CSF-specific OCBs.[15] Gray brackets represent statistical significance ($p < 0.01$) that was reproduced only in 1 of the independent cohorts (data not shown), whereas black brackets highlight those differences that reached statistical significance ($p < 0.05$) in each independent cohort based on the analysis of variance and Tukey's correction method for pairwise multiple comparisons. Dotted lines represent the upper limit of normal values (mean + 2 standard deviations) of HDs for IgG index and AlbQ. For CSF WBC/μl (NIH clinic laboratory) the NIH Clinical Center normal limit (≤ 5 cells/μl) was utilized in the figure. For CEL quantification, 0 was considered normal. Thick black bars represent the median for each diagnostic category. (B) The area under the receiver operation characteristic curves (AUCs) and 95% confidence intervals (CIs; in parentheses) based on binary outcome: with (OIND and all MS groups) versus without (HD and NIND) intrathecal inflammation.

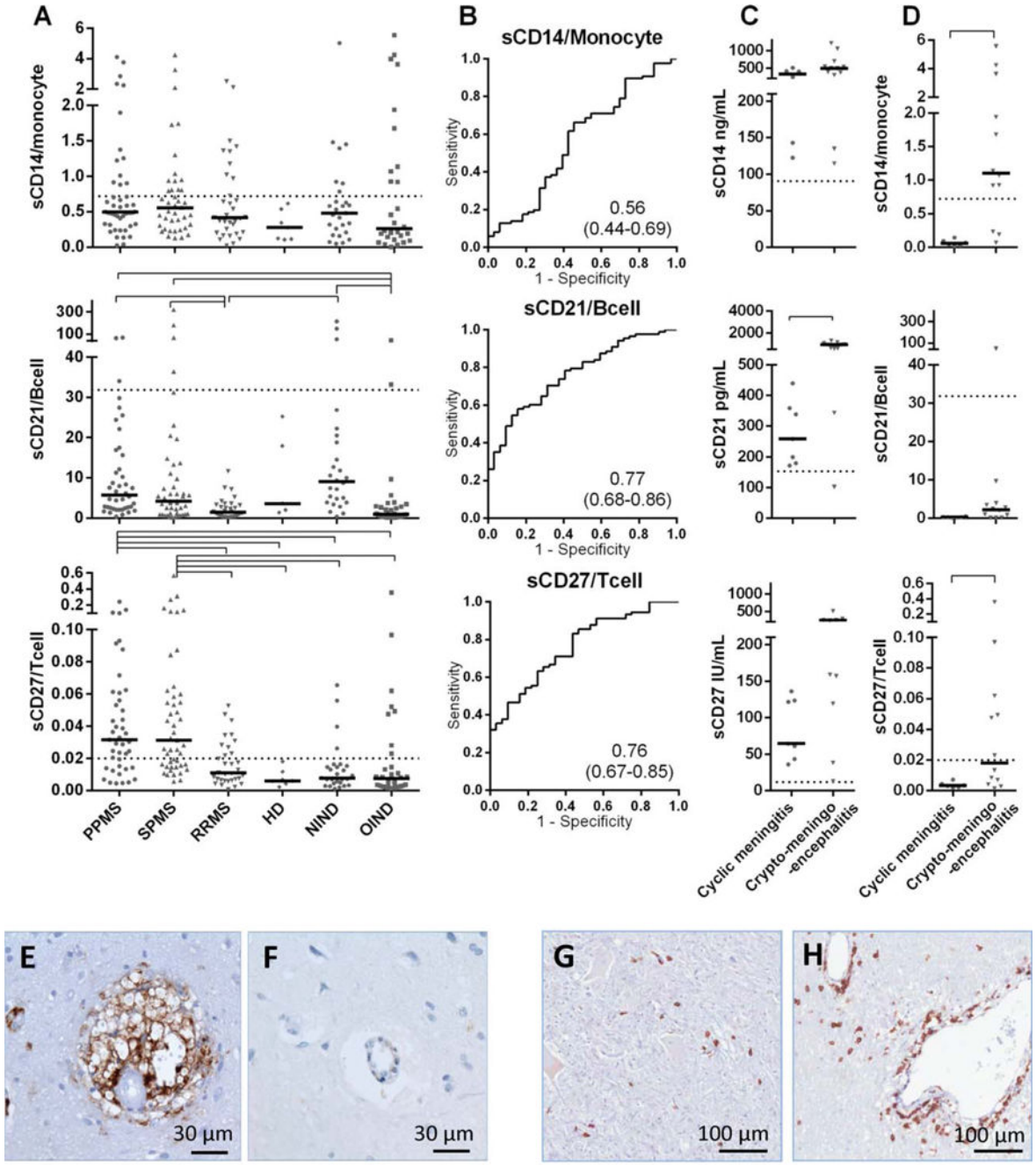

FIGURE 2.

FIGURE 2.

Combination of biologically related biomarkers. Three combinatorial biomarkers using Cohort B patients (the only cohort with available cerebrospinal fluid [CSF] immunophenotyping data) were calculated as ratios between the measured concentrations of cell-specific soluble CSF biomarkers and absolute numbers of corresponding CSF cells/ml of CSF (soluble [s]CD14/monocytes, sCD21/B cells, CD27/CD4+CD8 T cells). (A) Combinatorial biomarker levels in primary progressive multiple sclerosis (PPMS), secondary progressive MS (SPMS), relapsing–remitting MS (RRMS), healthy donors (HD),

noninflammatory neurological diseases (NIND), and other inflammatory neurological diseases (OIND) were compared between each diagnostic category. Dotted lines represent the upper limit of normal values, calculated as mean + 2 standard deviations of the HD cohort; thick black bars represent the median for each diagnostic category. Black brackets highlight statistically significant differences ($p < 0.05$) between diagnostic categories (PPMS, SPMS, RRMS, HD, NIND, and OIND) based on pairwise multiple comparisons with Tukey's correction. (B) Area under the receiver operation characteristic curves and 95% confidence intervals (in parentheses), where the binary outcome is defined as patients with progressive MS (who have elevated ratios and therefore likely more immobile cells in central nervous system [CNS] tissue) versus patients with RRMS (who have more mobile immune cells detectable in the CSF). (C) Results from measured concentrations of the cell-specific soluble CSF biomarkers sCD14, sCD21, and sCD27 for 2 homogeneous diagnostic subcategories of OIND: patients with cyclic meningitis (patients with cyclic aseptic meningitis without accumulation of neurological disability) and nonimmunocompromised patients with cryptococcal meningoencephalitis (patients with both CSF pleocytosis and accumulation of neurological disability). (D) Results from the sCD14/monocyte, sCD21/B-cell, and sCD27/T-cell ratios in the same 2 diagnostic subcategories of OIND patients. Thick bars represent cohort medians, and dotted lines represent upper limits of normal values (calculated as mean + 2 standard deviations from HD). Brackets highlight statistically significant differences ($p < 0.05$) between the 2 diagnostic categories based on 2-sample *t* test. (E–H) CNS autopsy tissue staining from a nonimmunocompromised cryptococcal meningoencephalitis patient (E, F) and a patient with undiagnosed CNS conditions, who was demonstrated to be neuroinflammatory based on autopsy results (G, H). (E) Brain tissue stained with anti-CD68 antibody showing accumulation of macrophages (brown) around a vessel. (F) Adjacent brain tissue stained with anti-CD3 antibody demonstrating a relative paucity of T cells. (G) Spinal cord tissue stained with anti-CD8 antibody showing invasion of $CD8^+$ T cells into the tissue. (H) Brain tissue stained with anti-CD8 antibody showing accumulation of $CD8^+$ T cells in perivascular space and their infiltration of brain tissue.

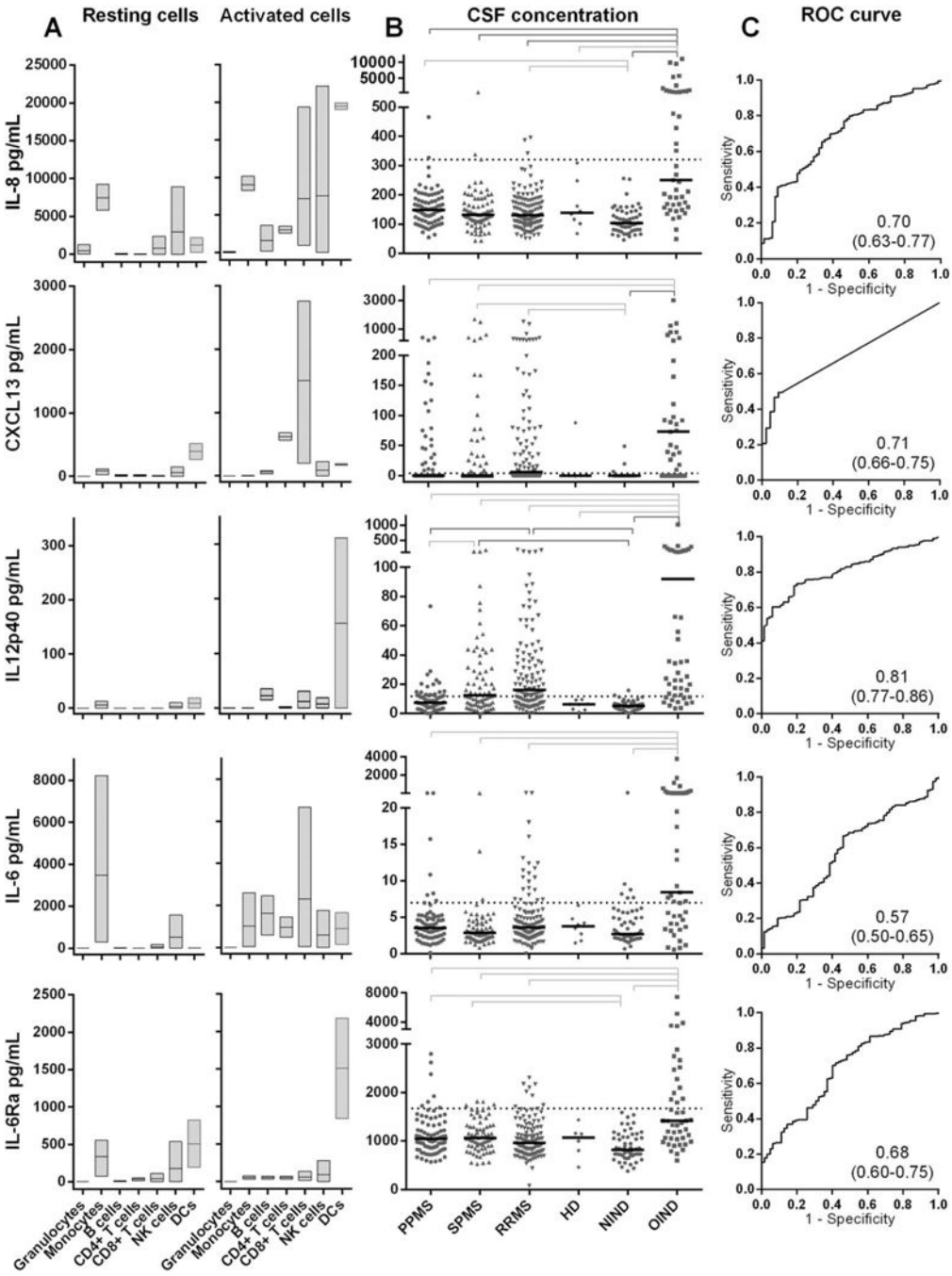

FIGURE 3.

Interleukin (IL)-12p40 and IL-8 are the most useful biomarkers of intrathecal inflammation among tested cytokines and chemokines. (A, B) Candidate biomarkers (IL-8, C-X-C motif chemokine 13 [CXCL13], IL-12p40, IL-6, and IL-6Ra) from the cytokine/chemokine category were quantified using commercially available or newly developed electrochemiluminescence sandwich immunoassays in cultured supernatants from purified, negatively selected immune subtypes (A) or coded cerebrospinal fluid (CSF) samples from combined Cohorts A and B (n = 386; B); 1×10^6/ml of purified granulocytes, monocytes, B

cells, $CD4^+$ and $CD8^+$ T cells, natural killer (NK) cells, and dendritic cells (DCs) from healthy donors (HD; n = 3) were either left untreated (A, left) or polyclonally stimulated with phorbol myristate acetate/Ionomycin (A, right) for 48 hours before collection of supernatants. Biomarker concentrations were recalculated per million cells of each specific subtype using flow cytometry data for purity of each seeded culture. In B, CSF biomarker concentrations in primary progressive multiple sclerosis (PPMS), secondary progressive MS (SPMS), relapsing–remitting MS (RRMS), HD, noninflammatory neurological diseases (NIND), and other inflammatory neurological diseases (OIND) were compared between each diagnostic category. Gray brackets represent statistically significant differences ($p < 0.01$) that were reproduced in only 1 of the cohorts, whereas black brackets represent those differences that reached statistical significance ($p < 0.05$) in both cohorts based on pairwise multiple comparisons with Tukey's correction method. Dotted lines represent the upper limit of normal values (calculated as mean + 2 standard deviations from HD); thick black bars represent the median for each diagnostic category. (C) Area under the receiver operation characteristic (ROC) curves and 95% confidence intervals (in parentheses), where the binary outcome is defined as with (OIND and all MS groups) versus without intrathecal inflammation (HD and NIND).

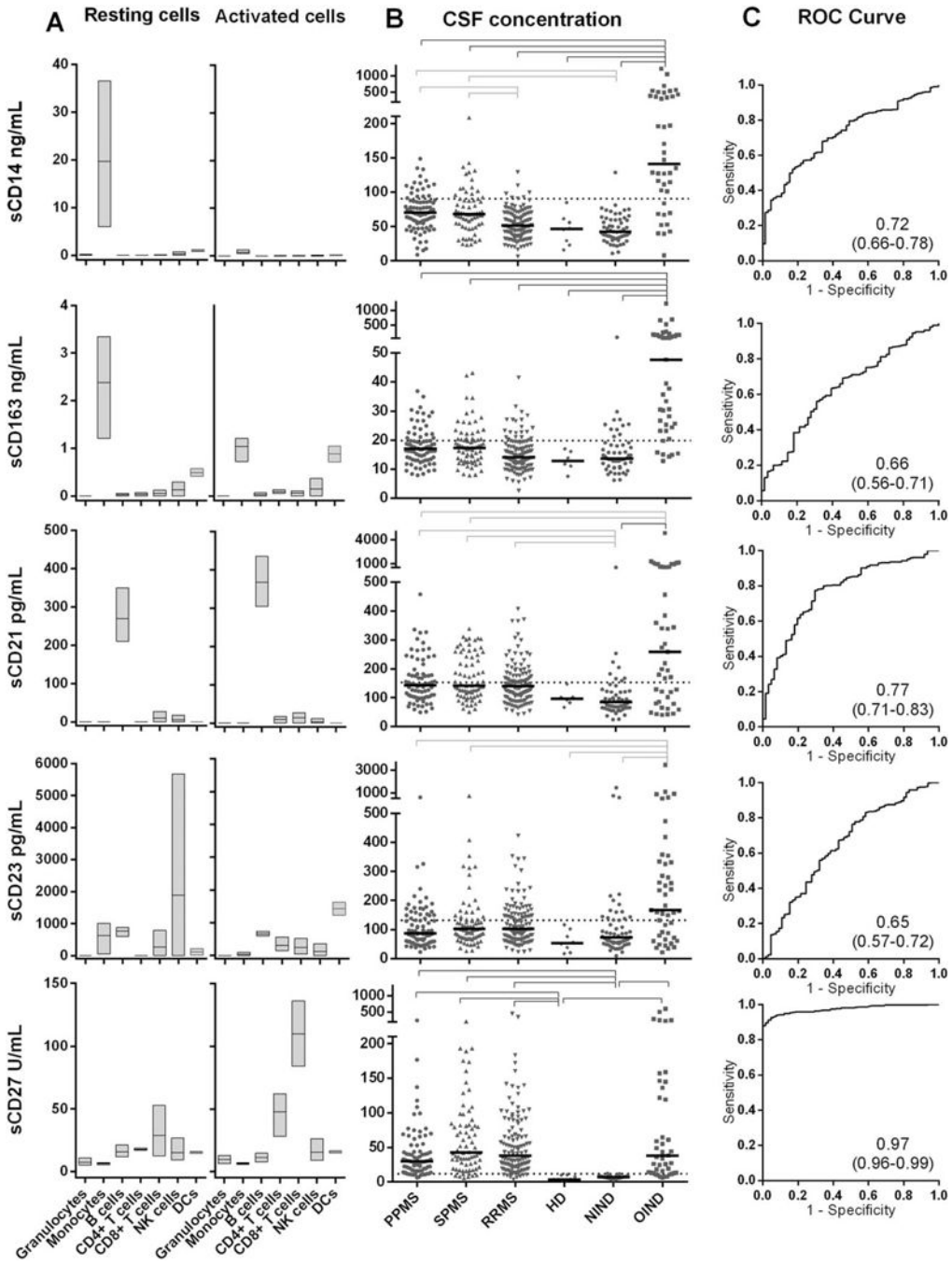

FIGURE 4.

Cell surface markers have more restricted cellular origin, and soluble (s)CD27 is an outstanding biomarker of intrathecal (T-cell–mediated) inflammation. (A) Candidate biomarkers (sCD14, sCD163, sCD21, sCD23, and sCD27) from cell surface markers were quantified using newly developed electrochemiluminescence sandwich immunoassays in cultured supernatants from purified, negatively selected immune subtypes or coded cerebrospinal fluid (CSF) samples from combined Cohorts A and B (n = 386; B); 1×10^6/ml of purified granulocytes, monocytes, B cells, $CD4^+$ and $CD8^+$ T cells, natural killer (NK)

cells, and dendritic cells (DCs) from healthy donors (HD; n = 3) were either left untreated (A, left) or polyclonally stimulated with phorbol myristate acetate/Ionomycin (A, right) for 48 hours before collection of supernatants. Biomarker concentrations were recalculated per million cells of each specific subtype using flow cytometry data for purity of each seeded culture. (B) CSF biomarker concentrations in primary progressive multiple sclerosis (PPMS), secondary progressive MS (SPMS), relapsing–remitting MS (RRMS), HD, noninflammatory neurological diseases (NIND), and other inflammatory neurological diseases (OIND) were compared between each diagnostic category. Gray brackets represent statistically significant differences ($p < 0.01$) that were reproduced in only 1 of the cohorts, whereas black brackets represent those differences that reached statistical significance ($p < 0.05$) in both cohorts based on pairwise multiple comparisons with Tukey's correction method. Dotted lines represent the upper limit of normal values (calculated as mean + 2 standard deviations from HD); thick black bars represent the median for each diagnostic category. (C) Area under the receiver operation characteristic (ROC) curves and 95% confidence intervals (in parentheses), where the binary outcome is defined as with (OIND and all MS groups) versus without intrathecal inflammation (HD and NIND).

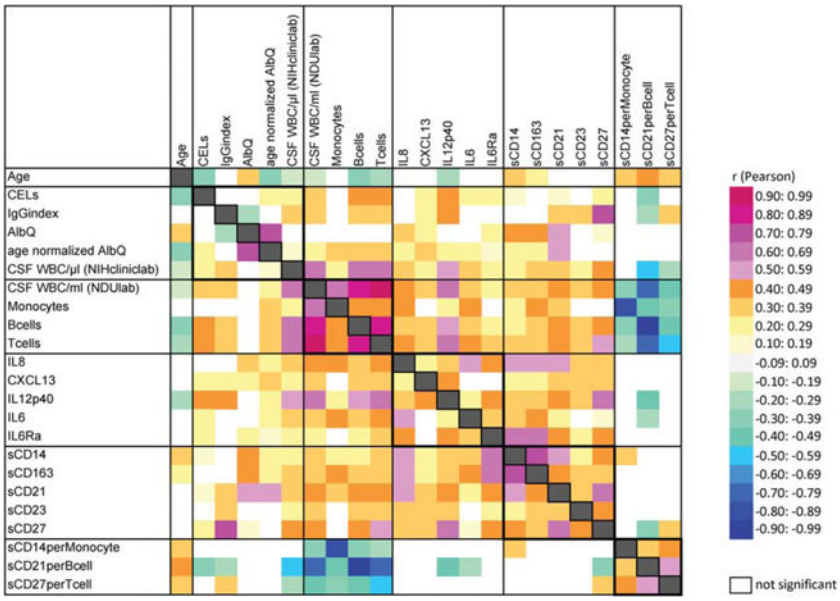

FIGURE 5.

Correlation matrix for all biomarkers. All biomarkers included in this study were analyzed with the Pearson correlation method. Only statistically significant correlations ($p < 0.001$ to account for multiple comparisons) are depicted with color, with strength of positive or negative correlation color-coded based on the provided heat map. Biomarkers were shown in groups as follows. Traditional biomarkers: the number of contrast-enhancing lesions (CELs) on brain magnetic resonance imaging performed at the time of lumbar puncture, immunoglobulin G (IgG) index, albumin quotient (AlbQ), age-normalized AlbQ, and white blood cell (WBC) counts per microliter in unspun cerebrospinal fluid (CSF) at the NIH Clinical Center. Enhanced cell counts: WBC counts per milliliter in CSF at the Neuroimmunological Diseases Unit (NDU) laboratory, absolute monocyte counts, B-cell counts, and T-cell counts. Cytokines and chemokines: interleukin (IL)-8, C-X-C motif chemokine 13 (CXCL13), IL-12p40, IL-6, and IL-6Ra. Soluble (s) cell surface markers: sCD14, sCD163, sCD21, sCD23, and sCD27. Calculated markers: sCD14 per monocytes, sCD21 per B cells, and sCD27 per T cells.

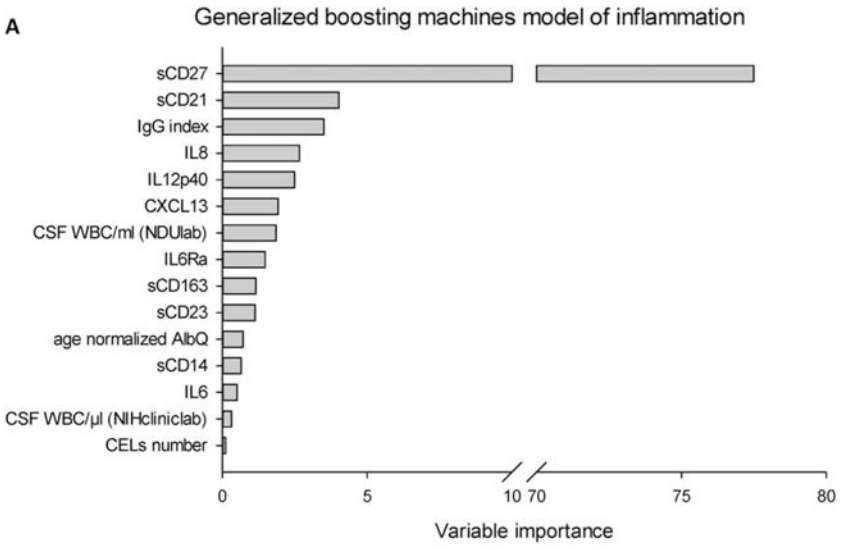

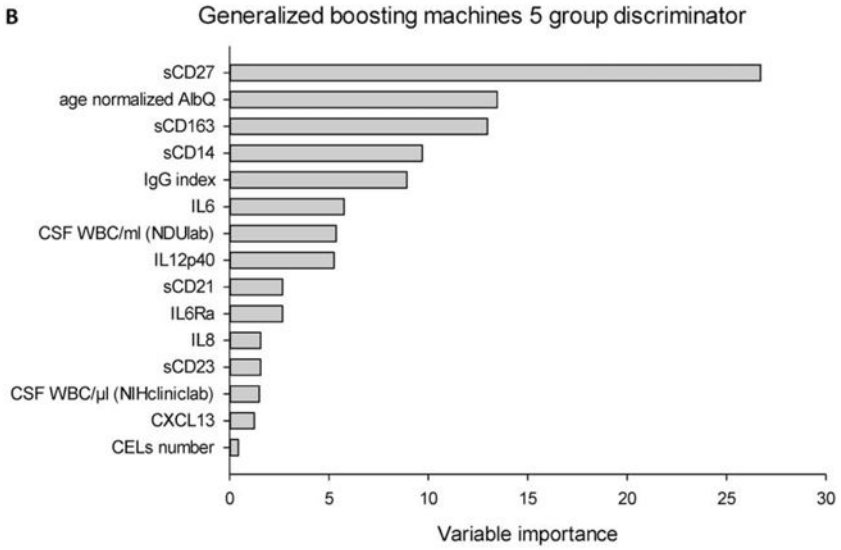

C

	Predicted category				
	HD+NIND	OIND	PPMS	RRMS	SPMS
HD+NIND	**31**	5	6	6	3
OIND	0	**7**	1	4	0
PPMS	0	0	**13**	17	7
RRMS	0	0	9	**45**	4
SPMS	0	1	7	16	**11**

FIGURE 6.

Ability of biomarkers to differentiate disease groups. Gradient boosting machines (GBM) results with cerebrospinal fluid (CSF) biomarkers are shown as plots of relative importance of biomarker variables. (A) In predicting presence versus absence of intrathecal inflammation, soluble (s)CD27 dominated the other variables in the classifier. (B) GBM variable importance results for 5 diagnostic categories. sCD27 was still the most important variable, but this time many additional variables contribute to predicting the response categories. (C) Confusion matrix for the validation cohort of the 5 diagnostic category GBM classifier. There were perfect predictions of noninflammatory neurological diseases (NIND)

+ healthy donors (HD) category, but misclassification of at least a few subjects from all remaining diagnostic groups, created by classifying new observations into the category with the highest predicted probability from the GBM. AlbQ = albumin quotient; CEL = contrast-enhancing lesion; CXCL13 = C-X-C motif chemokine 13; IL = interleukin; IgG = immunoglobulin G; NDU = Neuroimmunological Diseases Unit; OIND = other inflammatory neurological diseases; PPMS = primary progressive multiple sclerosis; RRMS = relapsing–remitting multiple sclerosis; SPMS = secondary progressive multiple sclerosis; WBC = white blood cells.

Ann Neurol. Author manuscript; available in PMC 2017 August 23.

TABLE 1

Demographics of Subjects

	Pilot Cohort A						Confirmatory Cohort]						All					
Characteristic	**PPMS**	**SPMS**	**RRMS**	**HD**	**NIND**	**OIND**	**PPMS**	**SPMS**	**RRMS**	**HD**	**NIND**	**OIND**	**PPMS**	**SPMS**	**RRMS**	**HD**	**NIND**	**OIND**
No.; F/M	36; 15/21	25: 11/14	88; 50/38	1; 1/0	30; 25/5	13; 5/8	45; 21/24	49; 32/17	33; 19/14	7; 3/4	27; 15/12	32; 10/22	81; 36/45	74; 43/31	121; 69/52	8; 4/4	57; 40/17	45; 15/30
Age, yr, median (range)	54 (42–66)	51 (29–66)	$_{38}ab$ (24–69)	29 (29–29)	$_{47}ac$ (11–66)	$_{51}c$ (23–63)	56 (31–70)	54 (28–66)	$_{41}ab$ (18–66)	40 (34–56)	$_{56}c$ (18–75)	$_{46}abd$ (3–75)	55 (31–70)	54 (28–66)	$_{38}ab$ (18–69)	$_{38}a$ (29–56)	$_{51}c$ (11–75)	$_{50}ab$ (3–75)
Disease duration, yr, median (range)	11.6 (1–38.2)	14.2 (1.2–41.8)	$_{2.6}ab$ (0–33)	n/a	$_{2.4}ab$ (0.3–17.8)	$_{2.7}b$ (0.92–12.8)	10 (1–38.8)	$_{24.1}a$ (1.4–43.5)	$_{1.6}ab$ (0.1–36.3)	n/a	$_{4.2}b$ (0.4–34.6)	$_{1.9}ab$ (0.4–7.8)	10.4 (1–38.8)	$_{21.3}a$ (1.2–43.5)	$_{2.1}ab$ (0–36.3)	n/a	$_{2.5}ab$ (0.3–34.6)	$_{2.2}ab$ (0.4–12.8)
EDSS, median (range)	6 (2–7.5)	6 (6–7)	$_{1.5}ab$ (0–5)	n/a	n/a	n/a	6 (2–6.5)	$_{6.5}a$ (2.5–7)	$_{2.5}ab$ (1–2.5)	n/a	n/a	n/a	6 (2–7.5)	$_{6.5}a$ (2.5–7)	$_{2}ab$ (0–5)	n/a	n/a	n/a
SNRS, median (range)	65 (45–94)	64 (45–75)	$_{92}ab$ (70–100)	n/a	n/a	n/a	68 (41–90)	$_{59}a$ (44–82)	$_{89}ab$ (77–98)	n/a	n/a	n/a	66 (41–94)	60 (44–82)	$_{91}ab$ (70–100)	n/a	n/a	n/a
IgG index, median (range)	0.66 (0.44–2.85)	0.72 (0.42–1.85)	$_{0.87}a$ (0.50–3.83)	0.46 (0.46–0.46)	$_{0.50}abc$ (0.38–0.61)	$_{0.55}c$ (0.47–0.70)	0.68 (0.42–3.52)	0.94 (0.45–3.62)	0.85 (0.55–2.81)	$_{0.53}abc$ (0.37–0.59)	$_{0.51}abc$ (0.42–0.62)	$_{0.62}bc$ (0.37–1.35)	0.68 (0.42–3.52)	0.76 (0.42–3.62)	0.85 (0.50–3.83)	$_{0.51}abc$ (0.37–0.59)	$_{0.5}abce$ (0.38–0.62)	$_{0.58}abcd$ (0.37–1.35)
Oligoclonal bands, +/− [%]	32/3 [91 %]	19/1 [95%]	50/7 [88%]	0/1 [0%]	$_{0/21}abc$ [0%]	$_{4/2}d$ [67%]	43/0 [100%]	44/2 [96%]	32/0 [100%]	$_{0/5}abc$ [0%]	$_{1/25}abc$ [4%]	$_{12/4}d$ [75%]	75/3 [96%]	63/3 [95%]	82/7 [92%]	$_{0/6}abc$ [0%]	$_{1/46}abcf$ [2%]	$_{16/6}abc$ [73%]
Age-normalized AlbQ, median (range)	1.51 (0.43–2.85)	1.72 (0.48–6.25)	1.69 (0.59–4.93)	1.37 (1.37–1.37)	1.22 (0.81–2.53)	$_{2.04}b$ (1.43–4.10)	1.20 (0.44–4.13)	1.39 (0.52–2.62)	1.50 (0.86–4.17)	1.70 (0.75–2.49)	1.45 (0.38–2.49	$_{3.01}abcde$ (0.54–14.30)	1.35 (0.43–4.13)	1.45 (0.48–6.25	1.63 (0.59–4.93)	1.54 (0.75–2.49)	1.27 (0.38–2.53)	$_{2.27}abcd$ (0.54–14.31)
Number of CELs, median (range)	0 (0–0)	0 (0–4)	$_{0.5}a$ (0–28)	n/a	$_{0}c$ (0–0)	0 (0–100)	0 (0–3)	0 (0–17)	$_{0}ab$ (0–15)	n/a	$_{0}c$ (0–0)	$_{2}abcd$ (0–20)	0 (0–3)	0 (0–17)	$_{0}ab$ (0–2.8)	n/a	$_{0}c$ (0–0)	$_{1.5}abd$ (0–100)

Disease duration, age-normalized AlbQ, and number of CELs were transformed by the Cox-box method. For oligoclonal bands, Fisher exact test and pairwise multiple comparisons with Bonferroni correction were used to evaluate the association between diagnoses. Age-normalized AlbQ was calculated with the following formula: (measured AlbQ)/(age normal AlbQ). Age normal AlbQ was calculated with the following formula: 4 + age/15.[16] Statistically significant differences in demographic and clinical parameters are noted with superscripts based on pairwise multiple comparisons with Tukey's correction method.

*a*Versus PPMS;

*b*versus SPMS;

*c*versus RRMS;

*d*versus NIND;

*e*versus HD.

*f*Positive oligoclonal band results but same number of bands between serum and CSF.

AlbQ= albumin quotient; CEL = contrast-enhancing lesion; EDSS = Expanded Disability Status Scale; F = female; HD = healthy donors; IgG = immunoglobulin G; M = male; n/a = not applicable; NIND = noninflammatory neurological diseases; OIND = other inflammatory neurological diseases; PPMS = primary progressive multiple sclerosis; RRMS = relapsing=remitting multiple sclerosis; SNRS = Scripps Neurologic Rating Scale; SPMS = secondary progressive multiple sclerosis.

TABLE 2

Methodological Details of Biomarker Measurements

Molecule	Manufacturer (antibodies/kit)	CSF Dilution Factor	Detection Limit[a]	Intra-assay Variation[b]	Interassay Variation[b]
IL-6	Meso Scale Diagnostics, Rockville, MD (K15049D)	1	0.74pg/ml	6.4%	9.6%
IL-6Ra	R&D Systems, Minneapolis, MN (MAB227,BAF227)	10	6.3pg/ml	2.2%	4.0%
IL-8	Meso Scale Diagnostics (K15049D)	1	0.53pg/ml	6.7%	9.8%
IL-12p40	Meso Scale Diagnostics (K15050D)	1	4.6pg/ml	6.5%	9.6%
sCD14	R&D Systems (MAB3833, BAF383)	100	0.49ng/ml	2.9%	6.8%
sCD21	R&D Systems (MAB4909, BAF4909)	2	5.8pg/ml	3.0%	6.8%
sCD23	R&D Systems (MAB1231, BAF123)	2	16.0pg/ml	4.0%	5.3%
sCD27	Sanquin, Amsterdam, the Netherlands (M1960)	20	0.4U/ml	2.3%	2.9%
sCD163	R&D Systems (MAB16071, BAM16072)	10	0.85ng/ml	2.7%	5.8%
CXCL13	R&D Systems (MAB801, BAF801)	1	17.4pg/ml	5.8%	8.8%
CD4	R&D Systems (MAB379, BAF379)	1	0.1ng/ml	Not detectable in the CSF	
CD8	Abnova, Taipei, Taiwan (H00000925-M10, PAB16612)	1	n/a	Not detectable in the CSF	
CD19	Abnova (H00000930-AP41)	1	1ng/ml	Not detectable in the CSF	
CD20	Abnova (H00000931-AP22)	1	1ng/ml	Not detectable in the CSF	
GM-CSF	R&D Systems (DY215)	1	10pg/ml	Not detectable in the CSF	
IFN-gamma	Meso Scale Diagnostics (K15049D)	1	0.6pg/ml	Not detectable in the CSF	
IL-7	R&D Systems (DY207)	1	10pg/ml	Not detectable in the CSF	
IL-10	Meso Scale Diagnostics (K15049D)	1	0.6pg/ml	Not detectable in the CSF	
IL-12p70	Meso Scale Diagnostics (K15049D)	1	0.6pg/ml	Not detectable in the CSF	

[a] When diluted CSF was used, detection limit was recalculated to reflect utilized concentration factor.

[b] Median value of concentration coefficient of variation.

CSF = cerebrospinal fluid; CXCL13 = C-X-C motif chemokine 13; IFN = interferon; IL = interleukin; s = soluble.